Journal of Nuclear Materials 390–391 (2009) 789–792

Contents lists available at ScienceDirect

Journal of Nuclear Materials

journal homepage: www.elsevier.com/locate/jnucmat

# A conceptual model of the magnetic topology and nonlinear dynamics of ELMs

T.E. Evans [a,*], J.H. Yu [b], M.W. Jakubowski [c], O. Schmitz [d], J.G. Watkins [e], R.A. Moyer [b]

[a] General Atomics, P.O. Box 85608, San Diego, California 92186-5608, USA
[b] University of California at San Diego, 9500 Gilman Drive, La Jolla, California 92093, USA
[c] Max Planck Institut für Plasmaphysik, EURATOM Association, Greifswald, Germany
[d] Forschungszentrum Jülich IEF4-Plasmaphysik, Association EURATOM-FZJ, 52425 Jülich, Germany
[e] Sandia National Laboratories, P.O. Box 5800, Albuquerque, New Mexico 87185, USA

ARTICLE INFO

*PACS:*
05.45.−a
05.45.Pq
28.52.−s
52.55.Fa
52.55.−s
52.55.Rk
52.25.Fi

ABSTRACT

A conceptual model is introduced describing the 3D magnetic topology and nonlinear evolution of Type-I edge localized modes (ELMs), which immediately follow the initial linear peeling-ballooning growth phase. The model requires feedback amplification of stable and unstable invariant manifolds that increases the helical perturbation. The amplification process is caused by a rapid growth of field-aligned helical thermoelectric currents that flow through relatively short pedestal plasma flux tubes connecting the inner and outer divertor target plates. It is shown that the model qualitatively agrees with the formation of global field-aligned emission filaments and with fast IR heat flux splitting patterns of the inner and outer strike points observed experimentally. In addition, the model predicts an increase in the size of the ELMs as the pedestal collisionality drops. Experimental data and modeling results are presented supporting the basic conceptual elements of the model.



## 1. Introduction and motivation

A conceptual model describing the dynamics of the edge plasma and the evolution of the pedestal magnetic topology following the linear growth phase of a peeling-ballooning instability [1], i.e., an edge localized mode (ELM), is presented. Understanding the physics, topology and dynamics of an ELM during its post-linear growth phase is essential for predicting the size of the instability versus the pedestal plasma conditions. In particular, a model is needed that can predict the temporal evolution of the plasma heat and particle distributions on vessel wall and divertor components.

Although ELMs are a common feature of stationary H-mode discharges in the current generation of tokamaks, there are significant gaps in our understanding of how these instabilities scale with the geometry of the plasma and operating conditions of larger tokamaks. Thus, there is an urgent need for a model that can be tested with experimental data from existing devices.

## 2. Conceptual description of the homoclinic tangle model for the evolution of ELMs

The fundamental process involved in the ELM model proposed here results from the transformation of the axisymmetric magnetic separatrix into a set of helical invariant manifolds by a small non-axisymmetric magnetic perturbation.

Topologically, the separatrix of an ideal poloidally diverted, single-null, tokamak is composed of a degenerate pair of invariant manifolds that belong to a hyperbolic fixed point of the system, typically referred to as an X-point in magnetic fusion plasma literature. As described in Ref. [2], in the absence of non-axisymmetric magnetic perturbations one of these invariant sets, referred to as a stable manifold, identically covers the other (unstable) manifold resulting in a topologically smooth separatrix. This is a generic property of a conservative system composed of unperturbed vector fields with a single hyperbolic point where the dynamics is described by integrating Hamilton's equations of motion. When sufficiently small perturbations are introduced the system remains Hamiltonian in nature and preserves its well-behaved (deterministic) dynamics. Such a system is commonly referred to as 'near integrable' and, generically, has a non-degenerate, transversely self-intersecting, separatrix manifold topology. These separatrix structures have been studied extensively in physics, mathematics, astrophysics, engineering and neuroscience where they are referred to as 'homoclinic tangles' [3,4]. Additionally, it is well known from the theory of conservative dynamical systems that the topology of these homoclinic tangles is 'the' fundamental element that dictates the behavior of the trajectories that form the solutions to the differential equations describing the dynamics of the system [4].

In a variety of tokamak plasmas, it has been shown that divertor heat flux and particle recycling patterns are consistent with

* Corresponding author.
*E-mail addresses:* evans@fusion.gat.com (T.E. Evans), moyer@fusion.gat.com (R.A. Moyer).

0022-3115/$ - see front matter © 2009 Elsevier B.V. All rights reserved.
doi:10.1016/j.jnucmat.2009.01.209

magnetic footprints produced by separatrix splitting associated with homoclinic tangles under some conditions [2,5,6]. Since homoclinic tangles result naturally from a variety of stationary and/or time-dependent non-axisymmetric magnetic perturbations that are found in any realistic tokamak, including toroidal field ripple, field-errors, MHD modes, control coils and small, spatially random components [2,5], it is not unreasonable to expect these structures to be the norm rather than the exception, whether in L-mode or in H-mode as well as between ELMs and during the onset of an ELM. It is the existence of a homoclinic tangle between ELMs that forms the basis for the model described below although the magnetic perturbation associated with the growth of the linear peeling-ballooning instability can also contribute to the non-axisymmetric seed field.

In the ELM model discussed here, it is assumed that the transient event is initiated when a peeling-ballooning mode is destabilized as the pedestal pressure gradient exceeds the linear marginal stability limit of the mode [1]. This produces an initial pulse of heat and particles that propagates radially outward into a small pre-existing homoclinic separatrix tangle. As the heat pulse intersects the tangle, near the foot of the pedestal in the outboard equatorial region, it is immediately conducted along an open helical flux tube connected to the divertor target plates by the high parallel thermal conductivity in the tube. Thus, the initial heat pulse arrives at the target plates well before the initial particle pulse and causes $T_e$ near the outer target plate to instantaneously increase relative to $T_e$ near the inner target plate due to a difference in the parallel connection lengths between these two targets and the outer equatorial plane.

The second stage of the ELM instability is initiated by the onset of a thermoelectric current driven between the outer and inner target plates due to the difference in $T_e$ between the two plates set up by the initial heat pulse described above. It should be realized that this current flows in the lobes of the tangle that penetrate into the outer pedestal region of the plasma. As the thermoelectric current grows it amplifies the small pre-existing homoclinic tangle at the foot of the pedestal. An example of the structure common to such a tangle at one point during its growth is shown in Fig. 1(a). Here, a poloidal cross-section of a tangle, produced by an $n = 3$ perturbation from a DIII-D non-axisymmetric control coil, illustrates the general topology of a pre-existing tangle although the toroidal mode number of the pre-existing tangle will vary depending on the source of the perturbation. It is noted that the tangle is biased toward the small major radius ($R$) side of the discharge. This bias is due to the lower field line pitch angle resulting from a higher toroidal magnetic field in that region compared to the large $R$ side of the discharge, i.e., $B_T \propto R^{-1}$. This effect produces more (unstable manifold) lobes extruding from the ideal separatrix on the high field side of the tangle than on the low field side, as shown in Fig. 1(a). Thus, as the thermoelectric currents begin to flow in the closed, short connection length ($L_c <$ electron collisional mean free path), ELM pre-filament flux tubes joining the two target plates they preferentially amplify the high field side lobes. As seen in Fig. 1(b), there are typically several short connection length flux tubes joining different parts of the magnetic footprints on the inner and outer target plates. These short flux tubes are indicated by the dark blue ($L_c \sim 500$ m) patches just above the X-point in Fig. 1(b). Thus, in addition to amplifying the lobes of the tangle these helical thermoelectric currents produce a spectrum of perturbations with various toroidal and poloidal mode numbers that drive resonant magnetic Poincaré islands on rational flux surfaces across the pedestal. As these islands grow and overlap, they enhance the magnetic stochasticity across the pedestal and increase the heat and particle transport into the tangle.

During the next step in the process, the original helical filament grows explosively as thermoelectric currents amplify the lobes of the homoclinic tangle and induced strong pedestal stochasticity. This process results in a self-amplification of the lobes due to a positive feedback loop between the size of the tangle lobes, an increasing stochastic layer width and an increase in the heat flux to the target plates driving the current. During this process, the tangle takes on the appearance of growing helical filaments that protrude beyond the edge of the plasma and seems to propagate radially outward. This process also produces a toroidal rotation of the filamentary lobe structures due to the fact that heat flux from deeper regions of the pedestal intersect lobes with progressively longer $L_c$ that have different toroidal phases and the pitch angles leading to an increase in the edge safety factor due to a loss of edge current during the ELM. A key feature of the processes involved up to this point is that there is no need to invoke field line tearing and reconnection in the evolution of the ELM. The entire process can be described using ideal MHD theory without invoking resistive or dissipative effects. At this point, most of the pedestal

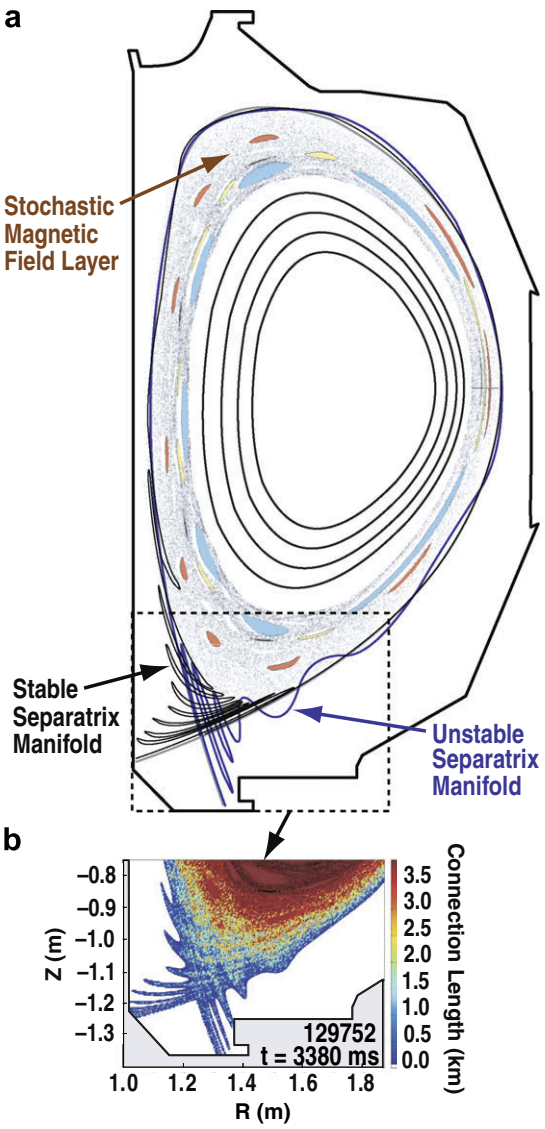


**Fig. 1.** (a) Conceptual illustration of a non-axisymmetrically perturbed DIII-D magnetic equilibrium showing a poloidal cross-section of the (un)stable branches of a homoclinic tangle shown in (black) blue and (b) calculated lengths of magnetic field lines that connect from the inner target plate region (45° and inner vertical wall) to the outer (horizontal) target plate through the hot plasma volume inside the separatrix manifolds.

energy (and particles) lost in the ELM crash has been transported to the divertors and walls through the growth of the filamentary tangle lobes.

In the final phase of the ELM crash, the temperature at some point across the pedestal drops enough for the plasma to become more collisional and resistive. At this point, two processes are envisioned to take over the dynamics and terminate the ELM crash. One involves the formation of resistive instabilities that separate the lobes of the tangle from the inner pedestal region. This shuts down the source of energy driving the thermoelectric currents and causes the lobes of the tangle to collapse back to their pre-ELM configuration. The second is a decrease in the electron collisional mean free path associated with the recycling and density rise in the divertor plasma, compared to the connection length of the filamentary lobes that reduces the parallel thermal conductivity and shuts down the heat flux to the target plates. This eliminates the $T_e$ gradients between the targets and turns off the thermoelectric currents, causing the lobes to collapse.

## 3. Supporting experimental observations

A number of experimental observations have been made on poloidally-diverted tokamaks that are qualitatively consistent with the model discussed above. In DIII-D, a line-filtered, fast visible camera viewing the low field side equatorial region of the plasma typically sees filamentary structures during L-modes as shown in Fig. 2. These emission filaments are also observed between ELMs in H-modes [7]. The structure, number and position of these emission filaments are consistent with those due to the presence a homoclinic tangle produced by any one of a number of non-axisymmetric perturbations as discussed above. Thus, these pre-ELM filaments represent the seed channels needed to produce the sequence of steps described by the ELM model in Section 2.

In MAST, images of the global topology of emission filaments observed during an ELM [8] are consistent with the helical structure produced by a homoclinic tangle. This can be seen by extending the lobes of the tangle shown in Fig. 1(a) around the surface of the plasma toroidally and comparing them with the filaments protruding from the upper x-point region of the MAST images showing the ELM filaments.

Other similarities between experimental observation of locked modes and ELMs are discussed in Ref. [9], where the first measurements of non-axisymmetric currents flowing between the divertor target plates during a series of ELMs are presented. An example of the toroidal distribution and temporal characteristics of these currents are shown in Fig. 3a–c along with a lower divertor $D_\alpha$ signal.

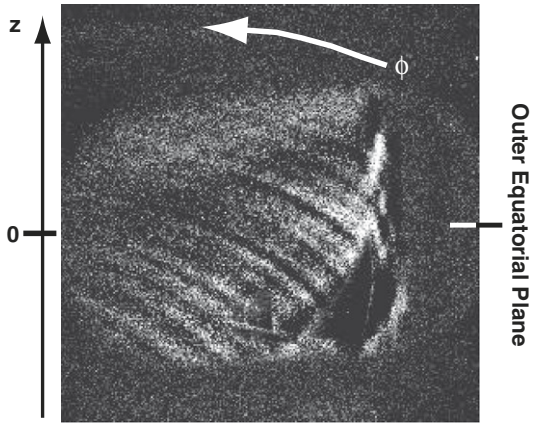


**Fig. 2.** Emission filaments observed with a line-filtered visible camera viewing the edge of DIII-D L-mode plasma near the low field side equatorial plane.

These currents are consistent in time and space with the thermoelectric currents [10] invoked in the model presented above. In the divertor, heat flux patterns observed during ELMs in ASDEX-U [11] are seen to have multiple striations that resemble the intersections of homoclinic tangle lobes with the target plates as seen in Fig. 1(b). Similar heat flux patterns are observed in DIII-D during ELMs as shown in Fig. 4.

## 4. Discussion and conclusions

A model based on the amplification of a small homoclinic tangle by thermoelectric currents flowing along the lobes of the tangle from one target plate to the other is particularly appealing, because it encompasses some of the temporal and spatial properties observed during the nonlinear evolution of ELMs observed experimentally and predicts others that have not yet been measured. In particular, the model predicts that the size of an ELM and its depth of penetration into the pedestal increases as the electron collisionality across the pedestal decreases. It also suggests that at low collisionality the fraction of the pedestal energy conducted to the divertors increases relative to the fraction of pedestal particles. In addition, the model incorporates an inherent bias toward higher ELM driven heat fluxes at the inner strike point compared to the outer strike point in high triangularity plasmas and has a natural tendency to produce higher toroidal mode numbers during the nonlinear growth of the ELM. As the pedestal collisionality is increased, the model produces smaller, higher frequency ELMs that are radially compressed near the foot of the pedestal. These may be related to the small Type-II or III ELMs observed at high collisionality. The model also provides a mechanism for a continued source of heat to the divertor targets during the entire nonlinear growth phase. Other models that have been proposed do not account for a continuous flow of heat to the target plates since the filaments detach from the pedestal as they grow.

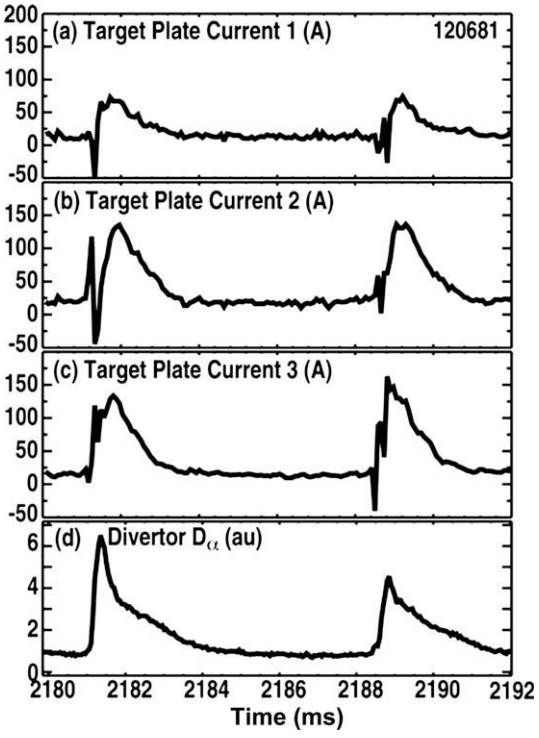


**Fig. 3.** Currents flowing between the lower divertor inner and outer target plates during ELMs in DIII-D at 3 toroidal angles: (a) 135°, (b) 180° and (c) 265°. A lower divertor $D_\alpha$ signal (d) is shown as a reference for the ELM timing.

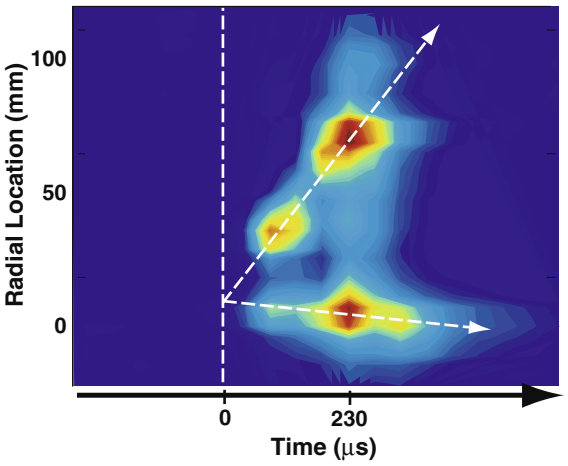


**Fig. 4.** Temporal evolution of the heat flux pattern measured during an ELM with a fast IR camera near the inner strike point in DIII-D. Red regions correspond to high heat flux. Here, the increase in the separation between the two striated footprints suggests a rotation and growth of the tangle lobes seen in Fig. 1.

In Section 3, it is argued that filament-like helical magnetic structures, illuminated by intermittent turbulent transport events in L-mode, are consistent with the topology of homoclinic tangles produced by magnetic perturbations known to exist in all real tokamaks. Since these filaments are also present between ELMs [7], they are the mechanism invoked in the model to explain the onset and development of the topological instability that is responsible for the nonlinear growth of the ELM. Although the model is intrinsically ideal in nature during the nonlinear growth phase (i.e., no field line tearing), tearing and reconnection may be involved in the terminal stage of the crash as discussed in Section 3. As discussed above and in previous publication [2,5], the model qualitatively agrees with some of the experimental observations currently available. Nevertheless, quantitative comparisons of the model with experimental data are still needed as well as modeling of the plasma properties in the lobes of the tangle in order to determine the size of the thermoelectric current and their effect on the size of the lobes. In conclusion, we note that the model predicts that the nonlinear growth of the ELM is intimately related to the size of the thermoelectric current flowing through the tangle. This suggests that by limiting this current flow with non-conductive or insulated target plates the dynamics of ELMs should be significantly modified on even suppressed.

## Acknowledgment

This work was supported by the US Department of Energy under DE-FC02-04ER54698, DE-FG03-07ER54917, and DE-AC04-94AL85000.

## References

[1] H.R. Wilson, S.C. Cowley, A. Kirk, P.B. Snyder, Plasma Phys. Control. Fusion 48 (2006) A71.
[2] T.E. Evans, R.K.W. Roeder, J.A. Carter, et al., J. Phys.: Conf. Ser. 7 (2005) 174.
[3] E. Simiu, Princeton Series in Applied Mathematics, Princeton University Press, Princeton, New Jersey, 2002.
[4] J. Guckenheimer, P. Holmes, Applied Mathematical Science, vol. 42, Springer-Verlag, New York, 1983.
[5] T.E. Evans, in: C. Chandre, X. Leoncini, G. Zaslavsky (Eds.), Chaos, Complexity and Transport: Theory and Applications, World Scientific Press, Singapore, 2008.
[6] T.E. Evans, I. Joseph, R.A. Moyer, et al., J. Nucl. Mater. 363–365 (2007) 570.
[7] J.H. Yu, G. Antar, J.A. Boedo, et al., in: Proceedings 34th EPS Conference on Plasma Physics, Warsaw, Poland, 2007.
[8] A. Kirk, G.F. Counsell, G. Cunningham, et al., Plasma Phys. Control. Fusion 49 (2007) 1259.
[9] T.E. Evans, C.J. Lasnier, D.N. Hill, et al., J. Nucl. Mater. 220–222 (1995) 235.
[10] G.M. Staebler, F.L. Hinton, Nucl. Fusion 29 (1989) 1820.
[11] T. Eich, A. Herrmann, J. Neuhauser, et al., Plasma Phys. Control. Fusion 47 (2005) 815.